Frequency-Dependent Electromechanics of Aqueous Liquids: Electrowetting and Dielectrophoresis

ARTICLE *in* LANGMUIR · APRIL 2004

Impact Factor: 4.46 · DOI: 10.1021/la035982a · Source: PubMed

3 AUTHORS, INCLUDING:

Kang L Wang
University of California, Los Angeles
968 PUBLICATIONS **17,502** CITATIONS
SEE PROFILE

Da-Jeng Yao
National Tsing Hua University
141 PUBLICATIONS **1,045** CITATIONS
SEE PROFILE

Frequency-Dependent Electromechanics of Aqueous Liquids: Electrowetting and Dielectrophoresis

T. B. Jones* and K.-L. Wang

Department of Electrical & Computer Engineering, University of Rochester, Rochester, New York 14627

D.-J. Yao

Institute of Microelectromechanical Systems, National Tsing Hua University, Hsinchu 30013, Taiwan

Received October 23, 2003. In Final Form: February 2, 2004

Electrowetting on dielectric and dielectrophoretic electromechanical mechanisms dominate microfluidic actuation in the low- and high-frequency limits, respectively. The frequency-dependent relationship between these two mechanisms has been clarified by the Maxwell stress tensor and a simple RC circuit model. In this paper, we report extensive height-of-rise measurements obtained with vertical, parallel, dielectrically coated electrodes to test this relationship using deionized water and solutions containing sugar and salt. For DC and AC (20 Hz to 20 kHz) voltage magnitudes up to ∼150 V-rms, the data are highly reproducible and, within experimental error, consistent with the square-law predictions of the model. Eventually as voltage is increased, a saturation phenomenon is observed which exhibits a weak dependence on frequency and is probably correlated to contact angle saturation.

Introduction

The laboratory on a chip and many other embodiments of μTAS (micro-total analysis systems) require some sort of microfluidic plumbing system to move and manipulate very small volumes of aqueous liquids. Electrical body forces exerted on liquids offer controllable means to achieve this function. Using microfabricated electrodes and the controlled application of voltage, the pumping and positioning of liquid masses, dispensing and mixing of subnanoliter droplets, and various two-phase separation operations have been demonstrated. Dielectrophoretic (DEP) and electrowetting on dielectric (EWOD) microactuation exemplify electromechanical mechanisms for transport and processing of sessile liquid droplets on a substrate. These schemes share the attractive attributes of very high actuation speed and relative geometric simplicity. Furthermore, their open structures obviate the sealing and leakage problems commonly encountered with closed channel microfluidic systems.

DEP actuation utilizes simple, coplanar electrodes patterned on a substrate, coated with a thin dielectric layer, and energized with AC voltage (200−300 V-rms at 50−200 kHz).[1] Rapid dispensing of large numbers of droplets as small as ∼10 pL[2] and a voltage-controlled array mixer[3] have been demonstrated using DEP. Joule heating can be a problem; however, a coated, metallic (Al) substrate underlying the electrodes serves as a heat sink and enables actuation of 1 mM KCl solutions.[4] EWOD microactuation uses somewhat similar, patterned electrodes, but typically with the liquid confined above by a transparent cover electrode.[5,6] In EWOD actuation, the water itself serves as a moving, deformable electrode. DC or low-frequency AC voltage, typically $<10^2$ V, is employed. Because the dielectric layer covering the electrodes blocks DC current, Joule heating is virtually eliminated. As a consequence, aqueous solutions with salt concentrations as high as 0.15 M can be actuated without heating.

A microfluidic system combining the open geometry and picoliter droplet dispensing capabilities of DEP microactuation with the lower voltage and frequency requirements and the conductive liquid handling capabilities of EWOD would represent a significant breakthrough. The basis of this statement is that such a system would offer geometric simplicity, good accessibility, and the unique droplet dispensing capabilities already demonstrated with DEP actuation.[2] Therefore, a prime motivation for our research has been to investigate the frequency-dependent relationship between the two mechanisms. In a previous paper, we introduced a simple electromechanical model that, in the low- and high-frequency limits, respectively, reduces to the EWOD and DEP mechanisms. This model was tested experimentally by measuring the frequency-dependent, electrically induced, excess pressure at an oil/water interface in a modified Quincke bubble apparatus.[7] We now report far more extensive experiments measuring the dielectric height-of-rise between parallel-plate electrodes as a function of frequency for various aqueous

(1) Jones, T. B.; Gunji, M.; Washizu, M. Dielectrophoretic liquid actuation and nanodroplet formation. *J. Appl. Phys.* **2001**, *89*, 1441−1448.

(2) Ahmed, R.; Hsu, D.; Bailey, C.; Jones, T. B. Dispensing picoliter droplets using DEP micro-actuation. In *First International Conference on Microchannels and Minichannels, Rochester, NY, April, 2003*; American Society of Mechanical Engineers: New York, 2003; pp 837−843.

(3) Gunji, M.; Jones, T. B.; Washizu, M. DEP-driven simultaneous 2 × 2 droplet array mixer. In *Micro Total Analysis Systems 2002: Proceedings of the μTAS 2002 Symposium, Nara, Japan, November, 2002*; Kluwer Academic: Dordrecht, 2002: Vol. 2, pp 721−723.

(4) Gunji, M.; Washizu, M. Liquid DEP droplet actuator and mixer on a heat-conducting substrate. Annual IEEE/IAS Conference, Little Rock, AR, June, 2003.

(5) Lee, J.; Moon, H.; Fowler, J.; Schoellhammer, T.; Kim, C.-J. Electrowetting and electrowetting-on-dielectric for microscale liquid handling. *Sens. Actuators* **2002**, *95*, 259−268.

(6) Pollack, M. G.; Fair, R. B.; Shenderov, A. D. Electrowetting-based actuation of liquid droplets for microfluidic actuation. *Appl. Phys. Lett.* **2000**, *77*, 1725−1726.

(7) Jones, T. B.; Fowler, J. D.; Chang, Y. S.; Kim, C.-J. Frequency-based relationship of electrowetting and dielectrophoretic liquid microactuation. *Langmuir* **2003**, *19*, 7646−7651.

10.1021/la035982a CCC: $27.50
Published on Web 03/03/2004

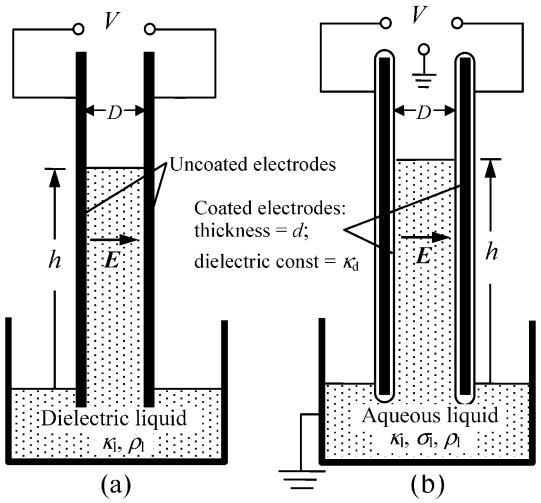

Figure 1. Dielectric height-of-rise apparatuses. (a) Pellat's original experiment demonstrating the electromechanical response of an insulating, dielectric liquid between parallel electrodes. (b) Modified apparatus for aqueous liquids using dielectric-coated electrodes. For modeling purposes, assume the two electrodes are electrically balanced, so that the midplane between them is at ground potential. In the experiments, AC voltage is supplied by a transformer with a center tap, which is grounded and connected to the metallic container holding the liquid.

solutions. This new apparatus is easy to use, and the reproducible data obtained with it have enabled a more thorough test of the predictive value of the electromechanical model in the frequency transition region, as well as in its low- and high-frequency limits.[8] In particular, it affords a good opportunity to test solutions of varied electrical conductivity.

Background

Over 100 years ago, Pellat used an apparatus similar to that depicted in Figure 1a to demonstrate that an insulating dielectric liquid rises upward between vertically oriented, parallel electrodes against gravity when a voltage is applied.[9] Let the electrically insulating liquid have mass density ρ_l and dielectric constant κ_l. If voltage V is applied between the electrodes at spacing D, the liquid responds by rising to height h above its equilibrium level. The so-called *dielectric height-of-rise* is[10]

$$h \approx \frac{(\kappa_l - 1)\epsilon_0 E^2}{2\rho_l g} \tag{1}$$

In eq 1, $E \approx V/D$ is the uniform electric field between the electrodes, $\epsilon_0 = 8.854 \times 10^{-12}$ F/m is the permittivity of free space, and $g = 9.81$ m/s^2 is the terrestrial gravitational acceleration. If H, w, and D are the height, width, and spacing of the electrodes, respectively, then eq 1 is accurate if $H \gg D$ and $w \gg D$. These inequalities ensure that the uniform field approximation is applicable.

Modified Pellat Apparatus

The following modifications to Pellat's height-of-rise experiment make the apparatus suitable for exploring the relationship between EWOD and DEP actuation: (i) the electrodes are coated with a dielectric layer of thickness $d \ll D$ and dielectric constant κ_d, (ii) the insulating, dielectric liquid is replaced by an aqueous medium, and (iii) variable frequency AC voltage is used. Refer to Figure 1b. The liquid has dielectric constant κ_l, electrical conductivity σ_l, and mass density ρ_l.

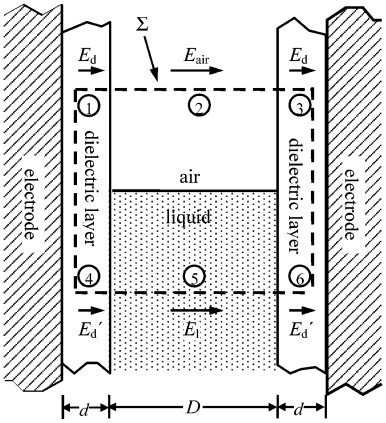

Figure 2. Definition of the closed integration surface Σ and associated area segments for determining the net vertical force of electrical origin on liquid between coated electrodes.

A closed surface integral of the Maxwell stress tensor is employed to determine the vertically directed, frequency-dependent force of electrical origin.[7]

$$F_z^e = \oint_\Sigma T_{zn}^e \, n_n \, dA \tag{2}$$

where n_n is the unit normal on the nth face of Σ. The stress tensor associated with the Korteweg−Helmholtz force density is[11,12]

$$T_{mn}^e = \epsilon E_m E_n - \delta_{mn}\frac{1}{2}\epsilon E_k E_k \tag{3}$$

In eqs 2 and 3, the Einstein summation convention is used and δ_{mn} is the Kronecker delta. Because it has no observable influence on the incompressible electrohydrostatics,[13] the electrostriction term is absent from eq 3.

According to the Korteweg−Helmholtz formulation, the vertical force components causing the liquid to rise act only at the liquid/air interface. Thus, the closed surface Σ must enclose this interface entirely. Figure 2 shows such a surface, with the top and bottom faces located far enough from the interface to avoid field distortion near the corners where liquid, air, and dielectric meet. Note that the details of the contact angle and the liquid profile near the contact line have no influence on the force calculation.

The surface integration reduces to a summation of the six enumerated area contributions identified in Figure 2. Expressions for the uniform, tangential electric fields at these surfaces, E_d, E_{air}, E_d', and E_l, may be determined using two simple RC circuit models, one above and the other below the liquid/air interface. Refer to Figure 3. The capacitance and conductance quantities, for convenience expressed per unit area, are $c_d = \kappa_d\epsilon_0/d$, $c_{air} = \epsilon_0/D$, $c_l = \kappa_l\epsilon_0/D$, and $g_l = \sigma_l/D$.

(8) Jones, T. B. On the relationship of dielectrophoresis and electrowetting. *Langmuir* **2002**, *18*, 4437−4443.

(9) Pellat, H. Mesure de la force agissant sur les diélectriques liquides non électrisés placés dans un champ élitrique. *C. R. Acad. Sci. Paris* **1895**, *119*, 691−694.

(10) Jones, T. B.; Melcher, J. R. Dynamics of electromechanical flow structures. *Phys. Fluids* **1973**, *16*, 393−400.

(11) Landau, L. D.; Lifshitz, E. M. *Electrodynamics of continuous media*; Pergamon: Oxford, 1960; Section 15.

(12) Woodson, H. H.; Melcher, J. R. *Electromechanical dynamics, part I: Discrete systems*; Wiley: New York, 1968; Chapter 7.

(13) Becker, R. *Electromagnetic fields and interactions*; Dover: New York, 1982; Section 37.

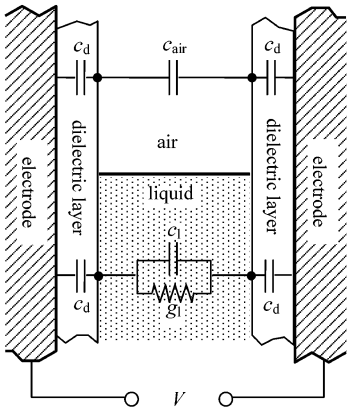

Figure 3. RC circuit model used to determine the frequency-dependent electric field expressions given in eq 4.

Let $V(t) = \mathrm{Re}[(\sqrt{2})Ve^{j\omega t}]$, where ω is the radian frequency and V is the root-mean-square value of the AC voltage. Using the circuit model, the rms electric field quantities are

$$E_d = \frac{c_{air}}{2c_{air} + c_d} V/d \tag{4a}$$

$$E_{air} = \frac{c_d}{2c_{air} + c_d} V/D \tag{4b}$$

$$E_d' = \mathrm{Re}\left[\frac{j\omega c_l + g_l}{j\omega(2c_l + c_d) + 2g_l} V/d\right] \tag{4c}$$

$$E_l = \mathrm{Re}\left[\frac{j\omega c_d}{j\omega(2c_l + c_d) + 2g_l} V/D\right] \tag{4d}$$

From eqs 2 and 3, the time-average force is

$$\langle F_z^e \rangle = w\left[-\kappa_d \epsilon_0 {E_d}^2 d - \frac{\epsilon_0 {E_{air}}^2}{2} D + \kappa_d \epsilon_0 {E_d'}^2 d + \frac{\kappa_l \epsilon_0 {E_l}^2}{2} D\right] \tag{5}$$

To determine the dielectric height-of-rise h, we set this z-directed (vertical) force of electrical origin equal to the net gravitation force pulling the liquid column downward.

$$\langle F_z^e \rangle = \rho_l g h w D \tag{6}$$

Bear in mind that the dielectric height-of-rise h in eq 6 is the *net* response of the liquid to the force of electrical origin.

Examination of eqs 4c and 4d reveals a critical frequency at

$$\omega_c = \frac{2g_l}{2c_l + c_d} \tag{7}$$

For $\omega \ll \omega_c$, $E_l \approx 0$, meaning that the liquid acts like a perfect conductor so that the entire voltage drop occurs in the dielectric layers. On the other hand, for $\omega \gg \omega_c$, the electric field below the liquid surface is nonzero and related by the electric flux continuity condition to the field in the dielectric layer: $\kappa_l E_l = \kappa_d E_d'$. Based on the critical frequency, low- and high-frequency limits for the height-of-rise may be identified.

$$h = \begin{cases} \dfrac{\kappa_d \epsilon_0 V^2}{4\rho_l g d D} & \omega \ll \omega_c \\ \dfrac{(\kappa_l - 1)\epsilon_0 V^2}{2\rho_l g D^2} & \omega \gg \omega_c \end{cases} \tag{8}$$

The low-frequency limit is identical to the result obtained using the contact angle model,[14] while the high-frequency expression agrees with eq 1 as long as $d \ll D$. Furthermore, it will be apparent that, at any fixed frequency, these expressions are identical to the perfectly conducting and perfectly insulating limits for the liquid, again respectively.[8]

Equations 4−6 combine to give a parabolic relationship between height-of-rise h and voltage V.

$$h = K^*(\omega) V^2 \tag{9}$$

where

$$K^* = \frac{\epsilon_0 {\kappa_d}^2 [{\epsilon_0}^2 \omega^2 (\kappa_l - 1)(\kappa_l d + \kappa_d D/2) + {\sigma_l}^2 d]}{4\rho_l g (2d + \kappa_d D)[{\epsilon_0}^2 \omega^2 (\kappa_l d + \kappa_d D/2)^2 + {\sigma_l}^2 d^2]} \tag{10}$$

Note that all material parameters and the frequency dependence are contained in the coefficient K^*. This expression is convenient when comparing the predictions of the model to the experiments.

Experiment and Results

The experiments were performed with an apparatus similar to that shown in Figure 1b. The parallel electrodes, made of 1 mm stainless steel, were of height $H = 65$ mm and width $w = 10$ mm. They were coated with parylene of thickness $d \sim 3.5 \pm 0.3$ microns and dielectric constant $\kappa_d = 3.1$. Short metal rods welded to each electrode (not shown in the figure) were used for mounting and positioning. All experiments were performed at fixed electrode spacing of $D = 1.0$ ($\pm$ 0.1) mm. Before conducting experiments, the electrodes were rubbed with insulating oil (MIDEL 7131), creating a thin film intended to reduce stiction and wetting hysteresis. This simple treatment greatly improved experimental reproducibility with no appreciable influence on the actual data. Without it, we observed hysteretic behavior; for example, the liquid would not return to $h = 0$ when the voltage was reduced to zero, leading to uncertainties of the order of millimeters in height-of-rise measurements. During experiments, the electrodes were usually dipped no more than 5 mm into the liquid in order to minimize any effects that imbalance of parasitic resistances might have on the voltage distribution.

The liquid was grounded through the aluminum channel, which had glass plates glued to the front and back for observation windows. AC voltage was generated by a function generator (Leader model no. LG 1301) connected to an amplifier (Krohn-Hite model no. DCA-50R) which was in turn used to drive a transformer with a grounded center tap. DC voltage was supplied by either a Fluke model no. 412B or Physik Instrumente model no. P263. All voltages were measured using a true-rms multimeter (Fluke model no. 87). Electrode gaps and height-of-rise values were measured with a long working distance microscope (Zeiss Stemi SV6) equipped with a CCD

(14) Welters, W. J. J.; Fokkink, L. G. J. Fast electrically switchable capillary effects. *Langmuir* **1998**, *14*, 1535−1538.

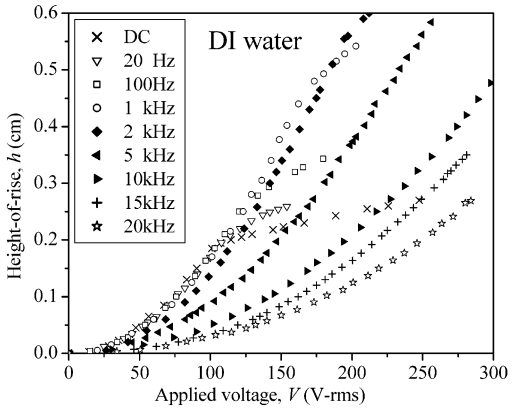

Figure 4. Frequency-dependent relationship of dielectric height-of-rise of DI water with conductivity 1.5×10^{-4} S/m for parallel electrodes spaced at $D = 1$ mm. Electrodes are covered with $d \approx 3.5$ microns of parylene, and then, to improve wetting uniformity, a very thin coating of insulating oil is applied. For lower voltages, the data show a quadratic dependence on voltage, while a saturation phenomenon becomes evident at higher values. For clarity, only selected frequencies are shown.

camera. Liquid conductivities were obtained with a YSI conductance meter (model no. 35).

The frequency dependence of dielectric height-of-rise was examined under DC voltage and AC from 20 Hz up to 20 kHz. In the conduct of the AC experiments, measurements were made both starting at low frequency and moving to higher values and from high frequency to low, the latter to minimize possible accumulation of trapped electric charge on the parylene. Figure 4 plots typical data for deionized (DI) water over the experimental range of frequencies. The largest height-of-rise values are observed for the lower frequencies and DC. The strongest dependence of h on frequency is registered in the range from ~2 to ~10 kHz. This is as expected because $\omega_c/2\pi =$ 5.2 kHz for DI water.

At any fixed frequency, the liquid rises steadily with voltage, generally following the square-law theory summarized in eq 9, up to some critical value where an evident deviation from parabolic behavior occurs. This behavior at higher voltages, presumably due to contact angle saturation, is considered further in the Discussion. If the voltage is decreased, the liquid drops back to the reference level with minimal hysteresis. Even after several rise−fall cycles, hysteretic effects are not particularly significant as long as the oil film is applied to the electrodes. Sometimes at higher voltages, the water surface drops abruptly, possibly due to breakdown through pinholes in the parylene layers.

Aqueous sugar (20 mM D-mannitol) and halide salt (1 mM KCl) solutions behave similarly. Because its conductivity is similar to that of DI water, the height-of-rise of mannitol exhibits strong dependence on frequency in the range from 2 to 20 kHz. On the other hand, the KCl solution data show virtually no frequency dependence because, with conductivity 100 times higher than that of DI water, the critical frequency is of the order of 480 kHz.

Figure 5a−c plots height-of-rise h versus V^2 for the three test liquids for voltages up to ~150 V-rms. Consistent with eq 9, these data are well correlated by straight lines. For a quantitative test of the theory, experimental values for the coefficient K were extracted from these figures by least-squares linear regression analysis. Figure 6 plots the values thus obtained for these coefficients versus frequency. The brackets on the data points reflect 99% confidence intervals for the K values. The solid lines are theoretical plots calculated from eq 10 using known

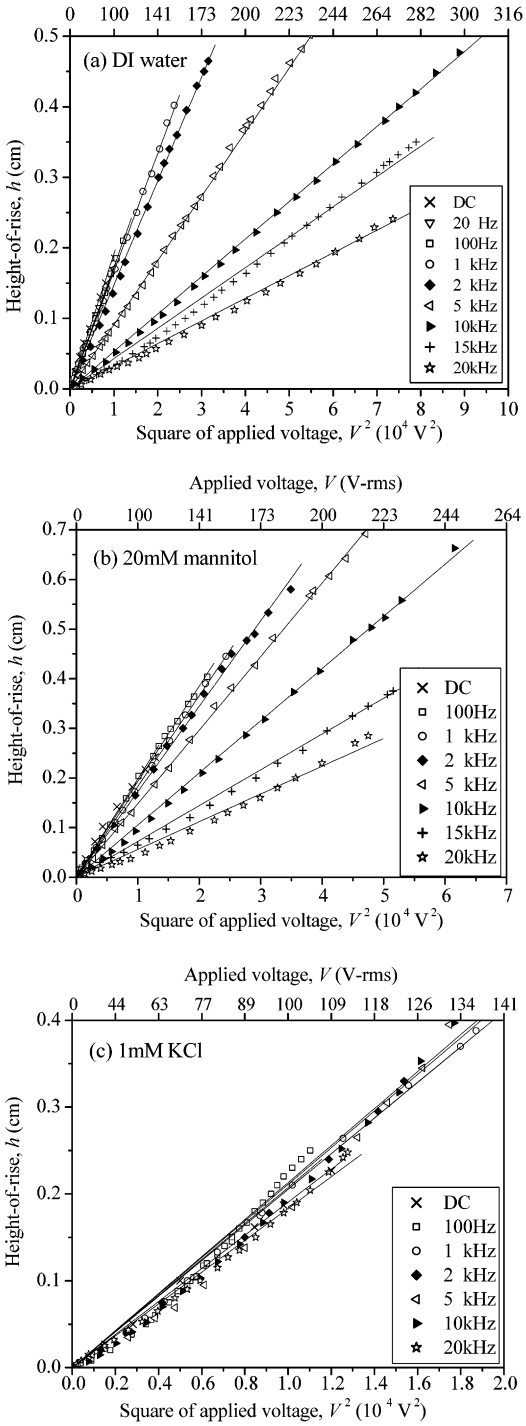

Figure 5. Height of rise h versus V^2 at lower voltages. The straight lines are least-squares regression fits carried out for each frequency. Coefficient K values obtained from these curve fits are compared with the theoretical K^* in Figures 6 and 7. (a) DI water with conductivity $\sigma_l = 1.5 \times 10^{-4}$ S/m; (b) 20 mM D-mannitol solution with conductivity $\sigma_l = 3.5 \times 10^{-4}$ S/m; (c) 1 mM KCl solution with conductivity $\sigma_l = 1.4 \times 10^{-2}$ S/m.

properties of the different liquids. The data correlate rather well to the theory. Note that each curve exhibits a low-frequency limiting value, corresponding to EWOD (or conductive) liquid actuation, and a high-frequency limit, corresponding to DEP (insulative) actuation. It is evident that the critical frequency of the more conductive KCl solution exceeds the 20 kHz limit of our AC supply.

As shown in Figure 7, the data may be consolidated by plotting the experimental K values from the least-squares

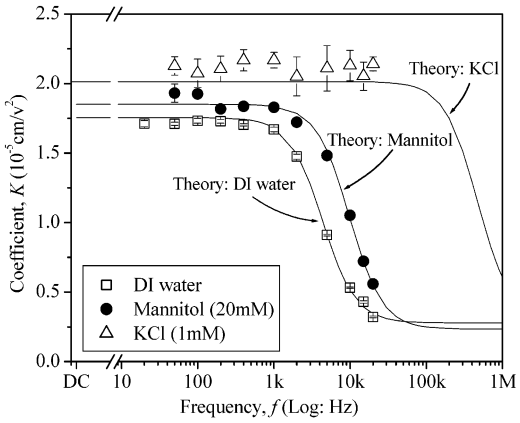

Figure 6. Frequency dependence of K for DI water, mannitol, and KCl. The error bars for data points signify 99% confidence intervals obtained using Student's t statistics, while the solid curves are calculated values of K^* from eq 10.

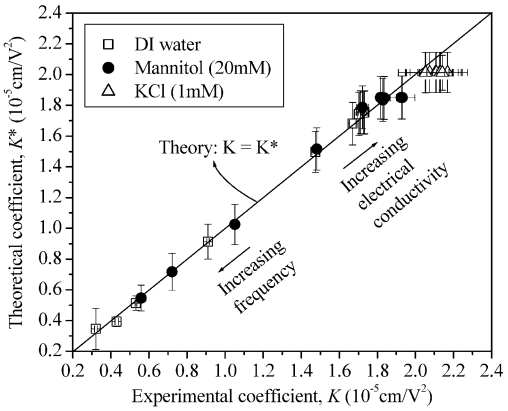

Figure 7. Composite plot of experimental K values from the least-squares curve fits versus theoretical coefficients K^* calculated from eq 10. Vertical error bars signify the uncertainties of the experimental parameters in eq 10, while horizontal bars indicate the 99% confidence intervals from Student's t statistics. To better understand the nature of this plot, the directions corresponding to increasing frequency and electrical conductivity are shown.

regression analysis versus calculated values of K^*. The horizontal error bars are the 99% confidence interval values from the linear regression analysis of the data. The vertical error bars reflect the uncertainty in the values for K^* calculated from eq 10. Standard sensitivity analysis was used to obtain these limits.

$$\Delta K^* = \left|\frac{\partial K^*}{\partial \omega}\right|\Delta\omega + \left|\frac{\partial K^*}{\partial \sigma_l}\right|\Delta\sigma_l + \left|\frac{\partial K^*}{\partial D}\right|\Delta D + \left|\frac{\partial K^*}{\partial d}\right|\Delta d \quad (11)$$

Table 1 summarizes the precision values of the most significant parameters, among which D and d dominate in determining the total uncertainty of K^*.

Within the limits of these uncertainties in the K and K^* values, the data in Figure 7 correlate successfully to theory, that is, $K = K^*$.

Discussion

For applied voltages below the saturation limit, the height-of-rise data agree remarkably well with the electromechanical model. This good agreement extends from DC to 20 kHz and covers aqueous liquid conductivities from $\sim 10^{-4}$ S/m (DI water and 20 mM mannitol solution) to $\sim 10^{-2}$ S/m ($\sim$1 mM KCl solution). The experimentally determined values for the frequency-dependent coefficient K agree with eq 10 to within $\pm$2% for DI water, $\pm$4.4% for D-mannitol solution, and $\pm$7% for KCl solution, at the 99% confidence level. All the data for the KCl solutions are consistent with the low-frequency limit, that is, $\omega \ll \omega_c$, for all test frequencies. This result is as expected because, for these conductive media, the critical frequency $f_c = \omega_c/2\pi = 480$ kHz exceeds the 20 kHz limit of our AC voltage source. It is evident that the operative mechanism for actuating biological media in practical microfluidic systems will be EWOD rather than DEP actuation.

Table 1. Estimates for Precisions of Essential Parameters Affecting Calculation of K^*

liquid	ω (s^{-1})	σ_l (10^{-4} S/m)	D (%)	d (%)	K^* (typical) (%)
DI water	$\pm$0.01	$\pm$0.5	$\pm$5	$\pm$2	$\pm$11
mannitol	$\pm$0.01	$\pm$0.5	$\pm$5	$\pm$2	$\pm$10
KCl	$\pm$0.01	$\pm$10	$\pm$5	$\pm$2	$\pm$6.5

Starting around 150 V-rms, the height-of-rise data start to deviate markedly from the parabolic dependence predicted by the model, that is, $h \propto V^2$. In similar experiments with DC voltages, using parallel-plate electrodes spaced at $D = 250$ μm, Welters and Fokkink reported a similar deviation from square-law behavior. They correlated the voltage at which the deviation occurred to independent measurements of the voltage at which contact angle saturation manifests itself.[14] It seems justified to make the hypothesis that the observed deviation from V^2 is likewise related to contact angle saturation; however, using AC voltage provides an opportunity to exploit frequency as a tool to study the nature of contact angle saturation and its influence on the electromechanical force. We have found that the voltage at which the deviation from square-law behavior manifests itself is weakly dependent on frequency. Furthermore, from Figure 4, it is evident that the transition from square-law behavior becomes less abrupt as the frequency is increased beyond $\sim$1 kHz. It is not clear whether this gradual change is directly connected to the critical frequency, which for DI water is $f_c = 5.2$ kHz. This frequency dependence, which Blake et al. might have been first to note,[15] is quite interesting and will be the subject of further investigation.

The linear theory of Buehrle et al. does not predict contact angle saturation.[16] This result seems entirely reasonable to us. Presumably, saturation is the consequence of some nonlinear, electrical dissipation mechanism that arises from the strongly intensified electric field in the vicinity of the liquid contact line. Such phenomena would most certainly exhibit a voltage threshold and might involve electrical corona,[17] the ejection of droplets from the sharp edge of the liquid layer,[18] or both in combination. One would expect the momentum imparted to ejected ions or droplets to influence the hydrostatics and dynamics of electrowetting. In particular, Mugele and Herminghaus have captured high-speed videos that show the formation

(15) Blake, T. D.; Clarke, A.; Stattersfield, E. H. An investigation of electrostatic assist in dynamic wetting. *Langmuir* **2000**, *16*, 2928−2935.

(16) Buehrle, J.; Herminghaus, S.; Mugele, F. Interface profiles near three-phase contact lines in electric fields. *Phys. Rev. Lett.* **2003**, *91*, 086101.

(17) Vallet, M.; Vallade, M.; Berge, B. Limiting phenomena for the spreading of water on polymer films by electrowetting. *Eur. Phys. J.* **1999**, *B11*, 583−591.

(18) Mugele, F.; Herminghaus, S. Electrostatic stabilization of fluid microstructures. *Appl. Phys. Lett.* **2002**, *81*, 2303−2305.

of large numbers of droplets, widely distributed in size, along the contact line.[19]

Conclusion

A simple theory based on a circuit model and the Maxwell stress tensor[7] has been used to determine the height-of-rise of a conducting liquid between parallel, coated electrodes. The high- and low-frequency limits of the resulting predictive relation are identical to the cases of perfectly insulating and perfectly conducting liquids, respectively. The perfectly insulating case is familiar as Pellat's classic experiment from over a century ago. The perfectly conducting limit corresponds to the so-called "electrowetting" phenomenon. The Maxwell stress tensor method makes no reference to details of the electric field, the distribution of induced electric surface charge, or the contact angle of the liquid at the electrode. As the frequency is raised, the force makes a steady transition from the locally intense field acting on free charge at the liquid/air interface to a ponderomotive force, which, according to the Korteweg−Helmholtz force density formulation, also acts at the interface. The goal of any electrodynamical formulation of translational electrical forces acting on liquids or solids is to determine the net *observable* force acting to move the center of mass of the liquid. The classical demonstration of this force is the height-of-rise effect. The electrically induced contact angle reduction is another *observable* phenomenon, a deformation of the surface caused by the locally intense, nonuniform electric field. It occurs simultaneously with and is related, though not in a causal way, to the height-of-rise.[20] Both effects are electromechanical in nature.

Others have recognized the usefulness of distinguishing between electrowetting and the height-of-rise phenomenon.[21−24] When polarization forces are present, it is understood that electrodynamics does not establish the physical location where electrical forces act. In fact, various formulations, all of them valid, place the polarization body force at *different* locations. Their mutual consistency is made evident when the Maxwell stress tensor associated with any of these alternative formulations is used in a consistent fashion to calculate the net force on a ponderable body; all lead to the same result for the experimentally observable, translational force. It is for this reason that attribution of translational motions acting on liquid masses to electric-field-mediated changes in the contact angle is unnecessary.

Acknowledgment. M. Washizu (Tokyo University), T. Blake (Eastman Kodak Co.), K.-H. Kang (Pohang University of Science and Technology, Korea), and B. Shapiro (University of Maryland) have provided useful insights on electrowetting and dielectrophoresis. L. Chen assisted with the early experiments, and P. Osborne fabricated the apparatus. C. Bailey and R. Ahmed helped with the parylene coatings, which were done at the Rochester Institute of Technology with essential guidance from A. Raisanen. The National Institutes of Health, the Center for Future Health of the University of Rochester, the National Science Foundation, and the Infotonics Technology Center, Inc. (NASA Grant No. NAG3-2744) supported this work.

LA035982A

(19) The research website of F. Mugele (University of Ulm, Germany) contains movie clips showing electric-field-driven formation and ejection of sessile droplets which can be viewed or downloaded: http://www.uniulm.de/uni/fak/natwis/angphys/deutsch/projektgruppen/mugele/elektrowetting_eng.html.

(20) Consider the thought experiment of placing a very thin dielectric membrane, having the same electrical properties as the liquid, on top of the rising liquid column in Figure 1b so that the liquid/air interface is constrained to be flat and horizontal, with $\theta_c = 90°$. Despite this constraint, the liquid can be expected to rise uniformly as V^2, presumably with no saturation observed. An even simpler thought experiment demonstrating the existence of the electromechanical force is to replace the liquid with a rigid, conductive slab of thickness D, again having the same electrical properties. There is no doubt that the same time-average force will act on this slab and pull it upward. Thus, it is apparent that changes in the solid/liquid contact angle are not necessary to achieve upward motion against gravity or, by extension, to actuate conductive liquid using dielectric-coated electrodes in a microfluidic scheme. The only requirement is that the electric field be somewhere nonuniform, so that displacement of the ponderable mass changes the capacitance.

(21) Digilov, R. Charge-induced modification of contact angle: The secondary electrocapillary effect. *Langmuir* **2000**, *16*, 6719−6723.

(22) Prins, M. W. J.; Welters, W. J. J.; Weekamp, J. W. Fluid control in multichannel structures by electrocapillary pressure. *Science* **2001**, *291*, 277−280.

(23) Beni, G.; Hackwood, S.; Jackel, J. L. Continuous electrowetting effect. *Appl. Phys. Lett.* **1982**, *40*, 912−914 (refer to footnote 8).

(24) Torkkeli, A. Droplet microfluidics on a planar surface. Ph.D. Thesis, Helsinki University of Technology, Espoo, Finland, 2003, VTT Publication No. 504 (refer to Chapter 3).